Chemical Physics Letters 482 (2009) 180–188

Contents lists available at ScienceDirect

Chemical Physics Letters

journal homepage: www.elsevier.com/locate/cplett

Submillimeter spectrum and analysis of vibrational and hyperfine coupling effects in $(HI)_2$

L.H. Coudert [a], S.P. Belov [b], F. Willaert [b], B.A. McElmurry [b], J.W. Bevan [b,*], J.T. Hougen [c]

[a] LISA, UMR 7583, CNRS/Universités Paris 12 et Paris 7, 61 Avenue du Général de Gaulle, 94010 Créteil Cedex, France
[b] Chemistry Department, Texas A&M University, College Station, TX 77843-3255, USA
[c] Optical Technology Division, National Institute of Standards and Technology, Gaithersburg, MD 20899, USA

ARTICLE INFO

Article history:
Received 27 July 2009
In final form 28 September 2009
Available online 1 October 2009

ABSTRACT

Observed rotational–vibrational transitions of HI dimer in the geared bending mode, centered at 511.9 GHz, are reported. This ~50 kHz spectrum was recorded using a co-axially configured pulsed jet submillimeter spectrometer and hyperfine structure of $R(J)$ and $P(J)$ transitions from the quadrupole moments of iodine nuclei are completely resolved for low-J transitions. Analysis of hyperfine patterns was carried out using a theoretical approach accounting for the large amplitude motion effects and hyperfine matrix elements within and between vibrational states. The submillimeter analysis is consistent with a vibrationally averaged ground state $R_{cm} = 4.56372(1)$ Å and average bending angle $\theta = 46.405(1)°$.

© 2009 Elsevier B.V. All rights reserved.

1. Introduction

$(HF)_2$, $(HCl)_2$ and $(HBr)_2$ have in many ways been considered as prototypical hydrogen bonded interactions and consequently their structure and dynamics have been the subject of extensive experimental and theoretical investigations [1–14]. However, there have been relatively few corresponding studies of $(HI)_2$ where such ground state information is significant in characterizing mechanisms associated with $(HI)_2$ photochemistry [15–17]. Although $(HI)_2$ has been the subject of theoretical calculations [18,19], and infrared matrix isolation studies [20–23], there have been no rotationally resolved infrared studies of this dimer until relatively recently [24,25]. These latter spectroscopic results were inconclusive regarding specifics of molecular dynamics. The potential of this dimer could be similar to other members of the homologous series having a barrier to tunneling interconversion and an L-shaped global minimum. Alternatively, the barrier could be below the ground state or even non-existent, thus being consistent in the latter case with a single global minimum and a symmetric dimer structure. Additionally, the previously investigated rovibrationally resolved 4.5 μm supersonic jet spectrum of HI dimer [24] was recorded with an instrumental resolution of only 30 MHz which unfortunately prevented effective resolution and analysis of the expected complicated iodine ($I = 5/2$) quadrupole substructure. Resolving such hyperfine substructure through analysis of the microwave spectrum of $(HI)_2$ or HI–DI would also be expected to be difficult to accomplish due to a non-existent or small permanent dipole moment. However, further characterization of the structure and dynamics in the ground state of $(HI)_2$ is possible through resolution of the hyperfine structure of transitions between the ground state and its lowest vibrational excited state that occur in its submillimeter spectrum [26]. The hyperfine structure of iodine containing molecules has been found to be intrinsically interesting because such molecules display a very large hyperfine quadrupole coupling that can be accurately measured giving quantitative information about molecular dynamics and structure. ICN, HI, and I_2 for example have eQq hyperfine coupling constants [27–29] of −2420, −1828, and −2980 MHz, respectively, orders of magnitude larger than that of $H^{35}Cl$ and about 500 times larger than the 4 MHz value in $^{14}NH_3$. Because hyperfine coupling effects are so large in these types of molecules, second-order quadrupole coupling effects [30] or $\Delta J = \pm 2$ hyperfine coupling matrix elements [29] must be taken into account in order to accurately reproduce such spectroscopic data.Large hyperfine effects attributable to its two iodine atoms are expected in the submillimeter spectrum of the HI dimer but are not known to have been analyzed and compared with experimental [1,10,13,31] and theoretical [1,32,33] investigations of the structure and dynamics of homologous members in the hydrogen halide dimers series $(HF)_2$, $(HCl)_2$, and $(HBr)_2$. Investigation of the submillimeter spectrum of the HI dimer is now reported allowing us to resolve for the first time its complicated iodine–iodine quadrupole structure and to spectroscopically characterize its ground and first excited vibrational states using high resolution spectroscopy. The submillimeter data is also analyzed [26] in order to elucidate the effects of the large quadrupole

* Corresponding author.
E-mail address: bevan@mail.chem.tamu.edu (J.W. Bevan).

0009-2614/$ - see front matter © 2009 Elsevier B.V. All rights reserved.
doi:10.1016/j.cplett.2009.09.098

coupling and its interaction with the geared bending vibrational motion. Furthermore, these precisely determined dimer parameters give further insight into the structure of the HI dimer.

2. Experimental

The vibrational–rotational transitions of HI dimer associated with the v_5 geared bending mode have been observed using a coaxially configured pulsed jet submillimeter spectrometer [34] with some modifications [14]. An OB-80 backward wave oscillator tube was used as the radiation source from 500 to 713 GHz. The molecular complex was produced in a supersonic jet with the adiabatic expansion of 2% HI in 98% Argon at a stagnation pressure of 2 atm absolute pressure. The output frequency of the BWO tube was scanned in 10 kHz steps (4 μs/step) through the line profiles with forward and return scanning and Doppler-displaced components recorded using an InSb liquid helium cooled bolometric detector using 400–900 co-additions to give an averaged 2 kHz frequency accuracy for linewidths of ~50 kHz as shown for a single quadrupole component (Fig. 1). A broadband prediction of the spectrum is expected to be complicated even when predicted at an effective temperature of 1.2 K. The measured data consisting of 345 lines centered around 510 GHz connecting the ground vibrational state and the first excited vibrational state of the dimer are given in Table 1. All observed transitions are *a*-type transitions with $K'_a = K''_a = 0$ and $\Delta J = \pm 1$. For the $R(0)$, $R(1)$, $R(3)$, $R(3)$, and $R(3)$ transitions, 24, 72, 54, 10, and 16 hyperfine components were measured, respectively. For the $P(1)$, $P(2)$, $P(3)$, and $P(6)$ transitions, 24, 71, 34, and 40 hyperfine components were measured, respectively.

3. Initial spectral analysis

The measured data were first fitted to a Hamiltonian for a linear molecule with inclusion of appropriate distortion, as was used previously for the HBr dimer [14]. Our fits included use of Pickett's SPFIT program [35] to a Hamiltonian $H = H_{VR} + H_Q$. The geared bending mode is characterized by the frequency, v_5, the rotational B constants determined for the ground and excited vibrational states. We added one centrifugal distortion term Δ_{JJ}, using the Watson centrifugal-distortion Hamiltonian written in the *A*-reduced I^r representation. In addition to the rovibrational Hamiltonian, we also included the ^{127}I nuclear electric quadrupole Hamiltonian H_Q, characterized by the quadrupole constant χ_{zz} for both identical iodine nuclei in both states. Each value was constrained to be equivalent to one another. The magnetic hyperfine structure arising from the two hydrogen atoms was neglected as it could not be resolved. The standard deviation of the fit was 80 kHz, large compared to the estimated 2 kHz frequency accuracy of the measured transitions and indicating that a more sophisticated Hamiltonian needs to be developed and this will be considered in the next section. The currently determined parameters are: $v_5 = 511931.440(9)$, with ground state B (MHz), Δ_{JJ} (kHz) and χ_{zz} (MHz) 378.299(2), 0.377(35), −389.997(34) and the corresponding excited state B (MHz), Δ_{JJ} (kHz) and χ_{zz} (MHz) 370.810(1), 0.296(20), −377.371(34).

Fig. 1 shows the Doppler-displaced components of the recorded spectrum of HI dimer for the $R(0)\ I', F' \leftarrow I'', F' : 3,3 \leftarrow 3,3$ transition. The measured center frequency of the transition is determined to be 512679.0404 MHz.

4. Theory

An approach is developed for calculating the observed submillimeter frequencies that accounts for the fact that the hyperfine coupling Hamiltonian has $\Delta J = \pm 2$ nonvanishing matrix elements within as well as between the two lowest vibrational states: the ground vibrational state and the first excited vibrational state of the geared bending motion. Expressions for the rovibrational and hyperfine coupling Hamiltonians to be used for these two states will be given using symmetry considerations. This involves choosing the coordinates used to parameterize the dimer as well as determining their transformation properties under the operations of the dimer symmetry group. These results will also be given as well as expressions for the Hamiltonian matrix elements using the same ideas as for a somewhat analogous monomeric system [36]. The strength of the quadrupole coupling and matrix elements of the hyperfine Hamiltonian within as well as between the two vibrational states will be considered in order to improve the accu-

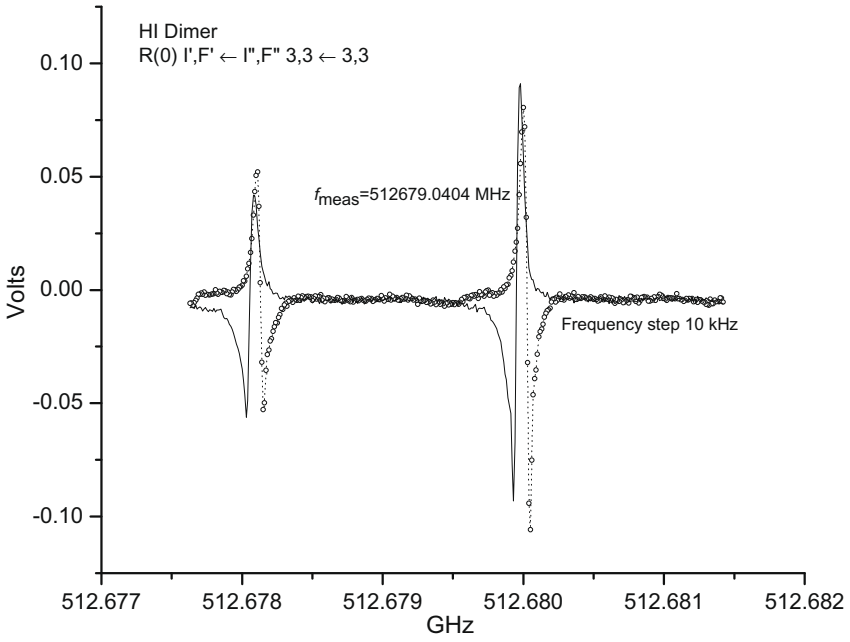

Fig. 1. Doppler-displaced components of one quadrupole component of the $R(0)$ transition.

Table 1
Assignments,[a] frequencies, and observed minus calculated differences in the rovibrational–hyperfine spectrum of the HI dimer.

F'	I'	F''	I''	Obs[b]	Diff[c]
				$R(0)$	
0	1	1	1	512557.1724	5
1	2	2	2	512565.4390	5
1	2	0	0	512569.9796	0
5	5	5	5	512579.0021	2
2	1	3	3	512584.5271	3
2	1	1	1	512589.9444	−2
3	2	4	4	512615.1986	0
3	2	2	2	512618.2403	−3
4	4	4	4	512633.2140	−5
4	3	3	3	512653.2445	−2
4	3	5	5	512657.1485	−4
3	3	3	3	512679.0404	−6
5	4	4	4	512688.9916	1
6	5	5	5	512714.5617	5
2	2	2	2	512714.8160	0
1	1	1	1	512739.3156	1
2	3	3	3	512748.1820	5
1	0	2	2	512748.3820	9
3	4	4	4	512751.8212	4
1	0	0	0	512752.9200	1
2	3	1	1	512753.5983	−1
3	4	2	2	512754.8620	0
4	5	3	3	512759.7410	4
4	5	5	5	512763.6443	1
				$P(1)$	
5	5	4	5	511081.8432	1
3	3	4	5	511085.4560	−7
2	2	3	4	511090.6880	−6
1	1	2	3	511092.3686	4
0	0	1	0	511093.3580	12
4	4	3	4	511093.5028	−12
3	3	2	3	511097.3826	−6
2	2	1	0	511097.5620	3
1	1	1	1	511107.2336	14
2	2	2	2	511132.1470	12
5	5	6	5	511132.6049	4
4	4	5	4	511158.3993	−5
3	3	3	3	511168.7351	6
5	5	4	3	511191.8096	11
3	3	4	3	511195.4241	6
4	4	4	4	511216.0261	2
2	2	3	2	511231.8977	5
4	4	3	2	511234.7140	0
1	1	2	1	511261.4816	1
3	3	2	1	511266.4948	−9
5	5	5	5	511272.6600	−5
0	0	1	2	511282.3440	−5
2	2	1	2	511286.5475	−15
1	1	0	1	511295.4247	−15
				$R(1)$	
5	5	4	5	513240.8662	26
3	1	2	3	513253.3503	11
2	0	1	0	513256.7110	17
1	1	1	1	513276.7870	26
0	2	1	0	513281.3123	39
4	5	4	5	513285.6935	−42
2	0	2	2	513291.2957	26
5	5	6	5	513291.6340	36
3	4	3	4	513293.4790	−46
2	3	2	3	513297.3035	−38
1	2	1	0	513299.3000	−24
6	5	6	5	513302.4349	−8
2	3	1	1	513312.1720	−25
4	4	5	4	513317.2872	12
5	3	4	5	513323.8235	2
3	1	3	3	513324.7028	23
1	3	2	3	513328.1095	−3
1	2	2	2	513333.8853	−14
3	4	2	2	513334.9376	−29
4	3	4	5	513341.7040	−8
4	2	3	4	513348.6793	1
5	5	4	3	513350.8284	33
3	1	4	3	513351.3870	18

Table 1 (*continued*)

F'	I'	F''	I''	Obs[b]	Diff[c]
5	4	5	4	513358.0029	−16
2	2	3	4	513359.2380	−1
2	2	1	0	513366.1134	9
2	3	3	3	513368.6592	−23
4	5	3	3	513368.9758	−26
4	4	4	4	513374.9145	20
3	3	2	3	513375.5493	7
3	2	3	4	513381.9205	−7
2	0	3	2	513391.0471	19
4	4	3	2	513393.6019	17
4	5	4	3	513395.6604	−31
2	2	2	2	513400.6990	19
6	4	5	4	513406.0227	1
2	4	3	4	513408.5846	−2
2	1	2	3	513410.1606	−11
3	5	4	5	513412.0470	8
4	2	5	4	513413.5750	7
2	4	1	0	513415.4625	10
5	4	4	4	513415.6308	−7
7	5	6	5	513415.9560	11
3	4	4	4	513416.0060	−28
3	1	2	1	513422.4619	7
3	2	2	2	513423.3801	11
2	1	1	1	513424.9880	−38
4	3	3	3	513425.0420	63
1	1	2	1	513431.0280	7
5	5	5	5	513431.6789	16
5	3	4	3	513433.6896*	−88
3	4	3	2	513434.6883	−36
6	5	5	5	513442.4909	−16
2	0	1	2	513445.6963	−1
3	3	3	3	513446.9046	22
2	4	2	2	513450.0442	16
4	3	4	3	513451.6703	2
1	1	0	1	513464.9776	−3
2	3	2	1	513466.4182	−39
0	2	1	2	513470.3002	24
4	2	4	4	513471.2032	16
3	3	4	3	513473.5923	21
4	5	5	5	513476.5113	−47
1	2	1	2	513488.2867	−40
4	2	3	2	513489.8900	12
3	5	3	3	513495.3220	17
1	3	2	1	513497.2220	−6
2	2	3	2	513500.4480	10
3	2	4	4	513504.4431	7
5	3	5	5	513514.6386	−6
3	5	4	3	513522.0055	11
4	3	5	5	513532.5205	−15
				$P(2)$	
2	1	3	3	510259.6870	−10
5	5	4	3	510272.9687	3
4	3	3	5	510278.3447	0
5	5	5	3	510291.2896	−10
4	4	3	2	510297.7890	−7
3	2	2	2	510303.1438	−18
3	3	3	5	510304.1402	−4
2	1	1	3	510308.6287	−13
3	2	4	2	510314.0551	−19
3	3	2	1	510318.4720	0
1	2	1	2	510319.6300	26
4	3	3	3	510328.4041	−14
5	5	4	5	510330.9150	51
4	4	4	2	510332.0730	−21
2	1	2	3	510340.6474	35
0	1	1	1	510344.2856	−15
2	2	2	4	510348.8211	1
4	3	4	3	510351.1160	−3
3	3	3	3	510354.2002	−18
1	2	2	0	510363.4707	−9
5	5	6	5	510366.0726	6
4	3	5	3	510369.4358	−17
3	2	3	4	510371.2550	44
2	3	3	5	510373.2740	−2
1	1	2	1	510373.3240	5
2	2	3	2	510376.3467	−2

Table 1 (*continued*)

F'	I'	F''	I''	Obs[b]	Diff[c]
3	3	4	3	510376.9123	−6
5	5	5	5	510376.9698	−25
1	0	2	4	510382.3860	9
6	5	7	5	510384.2610	1
4	5	3	5	510384.8398	4
2	1	3	1	510385.9332	−13
2	3	2	1	510387.6110	7
5	4	4	2	510387.8490	−18
3	4	2	4	510388.8692	3
4	4	3	4	510389.2718	41
4	4	5	4	510389.5310	6
5	4	6	4	510395.6537	−9
4	3	4	5	510409.0612	44
3	2	4	4	510413.5375	−18
3	2	2	0	510416.2700	−19
3	4	3	2	510416.3940	−1
2	3	3	3	510423.3403	−9
6	5	5	3	510426.8494	−8
4	4	4	4	510431.5538	−22
1	0	2	2	510433.2770	−15
4	5	3	3	510434.8586	−51
3	3	2	3	510435.1626	28
3	4	2	2	510439.7649	−16
5	4	5	4	510445.3080	11
3	4	4	2	510450.6765	−17
4	3	3	1	510454.6503	−17
4	3	5	5	510455.1163	−31
4	5	4	3	510457.6099	0
2	2	3	4	510467.8285	45
2	2	1	2	510469.0010	16
2	3	1	3	510472.2838	−11
4	5	5	3	510475.9320	−12
3	3	3	1	510480.4476	−20
1	1	2	3	510490.0193	38
6	5	6	5	510501.6327	9
1	0	1	2	510502.5670	24
2	3	2	3	510504.3019	36
3	4	3	4	510507.8780	48
6	5	5	5	510512.5325	−19
2	2	2	0	510512.8439	−18
4	5	4	5	510515.5584	50
1	1	1	1	510526.4310	−18
1	0	2	0	510546.4100	−9
2	3	3	1	510549.5873	−11
4	5	5	5	510561.6137	−25
				P(3)	
2	0	2	2	509565.4153	22
5	4	5	2	509569.7613	−26
3	2	3	2	509584.1584	−2
3	4	3	4	509585.2945	−13
4	3	4	3	509588.2146	−17
4	3	3	5	509588.9600	19
4	2	4	2	509589.0484	−2
4	4	4	4	509593.9590	35
4	5	4	5	509594.7249	−16
6	5	7	5	509596.1720	0
3	5	2	5	509601.8828	−1
7	5	8	5	509605.2196	1
5	5	5	5	509607.0095	34
2	1	3	1	509607.5571	4
1	2	2	2	509608.0040	−19
1	3	2	3	509608.4540	25
3	4	2	2	509609.0570	−33
5	4	6	4	509609.1923	1
3	3	4	3	509610.1320	−3
2	4	3	2	509610.8213	1
6	4	7	4	509612.0282	−13
5	3	5	3	509612.1360	1
0	2	1	2	509613.2662	15
4	4	5	4	509616.1407	−7
1	1	2	1	509616.4670	2
6	4	5	2	509617.8220	32
6	5	5	5	509617.8220	3
3	1	4	1	509617.8746	2

Table 1 (*continued*)

F'	I'	F''	I''	Obs[b]	Diff[c]
2	0	3	0	509618.1209	5
5	3	6	3	509620.8956	−10
3	5	3	1	509621.3511	5
2	3	3	3	509621.6676	−17
5	5	6	5	509622.2841	5
4	2	5	2	509625.3321	−5
				R(3)	
3	1	3	3	514779.7580	26
3	2	3	4	514781.1661	15
5	1	4	5	514781.8786	17
4	0	5	2	514782.0730	−31
4	4	4	4	514782.3252	29
3	4	4	2	514782.6226	−47
2	4	1	4	514788.3318	−51
2	2	2	2	514787.9392	15
4	0	3	4	514797.2358	7
5	5	5	5	514797.8310	16
3	4	2	4	514799.1413	−11
6	5	5	5	514799.7047	17
5	3	4	3	514801.3860	−51
1	4	1	4	514801.4375	28
5	2	4	2	514802.5260	3
2	4	2	4	514802.5760	8
6	2	5	2	514803.5255	−9
4	3	3	3	514803.4650	1
5	4	4	4	514804.2766	12
6	3	5	3	514804.7390	−7
3	2	2	2	514804.9275	−6
3	5	3	5	514805.6900	−5
4	1	3	1	514805.8030	10
4	2	3	2	514806.3306	12
7	3	6	3	514806.4578	−8
1	3	1	3	514806.9580	0
5	5	4	1	514808.1380	−2
4	4	3	0	514809.0440	−2
3	3	2	3	514809.2990*	−263
8	4	7	4	514809.5168	−2
3	3	2	3	514809.5740	12
0	4	1	4	514809.6914	−1
2	2	1	2	514811.1900	−12
6	4	5	4	514812.9557	−2
1	5	2	5	514813.4993	19
7	4	6	4	514813.8100	1
6	5	6	5	514814.9750	−17
7	5	6	5	514815.8240	−4
8	5	7	5	514823.4899	−1
4	5	4	5	514825.4938	−2
5	4	5	4	514826.4632	−26
3	2	4	4	514830.9165	9
3	4	3	4	514834.0741	−7
2	4	3	4	514837.5024	6
5	2	5	2	514838.8080	−2
5	1	5	5	514838.9970	6
2	5	3	5	514841.5600	16
6	2	6	4	514842.9574	19
4	1	4	3	514843.0130	9
5	3	5	3	514843.2320	0
4	3	4	1	514843.6250	−29
4	0	4	4	514846.9866	2
3	4	2	2	514857.8363	−27
3	2	3	0	514857.6334	−23
				R(4)	
3	5	2	5	515455.5056	−8
2	5	1	5	515455.9732	−15
4	1	4	3	515466.6867	30
3	3	3	3	515472.6402	9
5	3	4	5	515473.1340	13
6	1	5	1	515480.9233	8
8	5	7	5	515497.8212	−2
9	5	8	5	515500.3602	4
8	4	8	4	515451.3814	−23
8	5	8	5	515451.9509	34

(*continued on next page*)

Table 1 (*continued*)

F'	I'	F''	I''	Obs[b]	Diff[c]
				$P(6)$	
4	5	3	5	507128.5750	−17
5	5	5	3	507129.0190	5
7	3	7	3	507130.4615	−20
5	3	5	5	507130.9973	3
4	3	4	5	507131.0850	8
6	1	5	3	507132.1530	25
7	2	7	2	507132.5220	−17
6	1	6	3	507137.2364	7
6	5	7	1	507138.9910	−15
4	3	5	5	507140.9197	−2
7	5	7	1	507141.1222	−8
6	5	6	5	507145.0647	20
7	5	6	5	507147.1900	21
9	5	9	3	507147.3000	−28
3	5	3	5	507152.4120	−8
2	5	2	5	507154.3205	−6
1	5	1	5	507156.5465	−4
7	4	7	4	507160.5370	14
9	5	10	5	507160.8584	−5
8	3	8	3	507161.3756	1
10	5	11	5	507162.0253	−1
5	1	6	1	507164.0046	−2
5	2	6	2	507164.0046	5
8	5	9	5	507164.3679	−4
5	4	6	4	507170.7507	0
3	4	4	4	507171.4921	−2
6	5	7	5	507172.3256	3
6	1	7	1	507173.1531	−13
5	3	6	3	507174.4456	−13
5	5	6	5	507176.0922	0
1	5	2	5	507177.9672	16
2	5	3	5	507183.3688	12
3	5	4	5	507184.1085	4
5	5	5	1	507187.1737	−23
9	4	9	4	507204.0829	22
9	5	9	5	507212.7842	−27
7	3	7	1	507225.4484	−22
6	3	6	3	507226.6686	10
5	1	5	5	507227.9408	34
10	5	10	5	507248.2484	29
				$R(6)$	
10	5	10	5	516762.2791	22
4	5	3	5	516793.4151	−8
3	5	2	5	516795.0404	−8
5	5	4	5	516795.9853	−5
6	5	5	3	516799.1618	−1
9	5	9	5	516796.4416	−5
2	5	1	5	516799.7684	−2
10	4	9	4	516810.2042	0
11	5	10	5	516813.8211	2
10	5	9	5	516814.2033	−2
8	4	8	4	516816.4946	−19
3	4	3	4	516820.6644	15
3	5	3	5	516824.0894	11
4	5	4	5	516825.1123	5
7	5	7	5	516831.6492	−12
8	1	8	5	516836.3534	2

[a] Hyperfine components are assigned with F and I. The lower and upper states are the ground and $v_5 = 1$ states, respectively.

[b] Obs is the observed frequency of the rovibrational–hyperfine transition in MHz. An asterisks indicates transitions excluded from the analysis.

[c] Diff is the observed minus calculated frequency in kHz corresponding to the constants in Table 5.

racy in the energy level calculation. In this calculation, the magnetic hyperfine structure due to the two hydrogen atoms is ignored.

4.1. Internal coordinates and symmetry considerations

As illustrated by Fig. 2, the two hydrogen atoms of the HI dimer will be labeled 1 and 2, and the corresponding iodine atoms will be labeled *a* and *b*. It is then convenient to refer to the HI molecule containing atoms 1 and *a* (2 and *b*) as monomer 1 (2). In addition to the usual Eulerian type angles: χ_d, θ_d, ϕ_d, six internal coordinates are necessary to describe the HI dimer. They involve two bending angles θ_1 and θ_2, one torsional angle ϕ, and three distances R, r_1, and r_2. The equation relating the laboratory-fixed Cartesian coordinates to the molecule-fixed coordinates is the following:

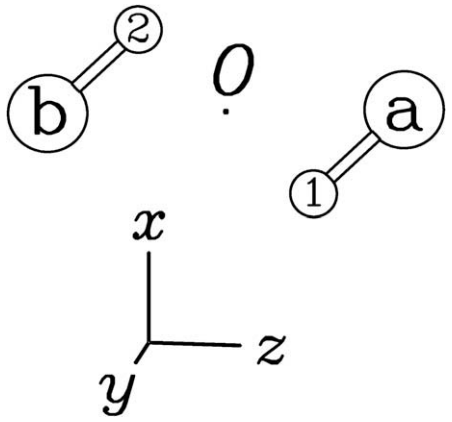

Fig. 2. Atom configuration for the HI dimer. A value of 43 and 137° is taken for the two bending angles θ_1 and θ_2, respectively. The torsional angle ϕ is set to 180°. The molecule-fixed *xyz* axis system is drawn below the molecule for clarity. Its origin is the molecule center of mass indicated by point *O*. This configuration with C_{2h} symmetry is the minimum of the dimer potential energy surface [38,39].

$$\mathbf{R}_i = \mathbf{R} + S^{-1}(\chi_d, \theta_d, \phi_d) \cdot \mathbf{a}_i(\theta_1, \theta_2, \phi, R, r_1, r_2). \quad (1)$$

In this equation, $\mathbf{R}_i$ and $\mathbf{R}$ are column vectors containing the three laboratory-fixed components of the position of atom i and the position of the molecular center of mass, respectively; the $\mathbf{a}_i(\theta_1, \theta_2, \phi, R, r_1, r_2)$ are a set of positions for the atoms which depend explicitly on the six internal coordinates; and $S(\chi_d, \theta_d, \phi_d)$ is the direction cosine matrix [37]. The positions $\mathbf{a}_i(\theta_1, \theta_2, \phi, R, r_1, r_2)$ are defined with the help of various rotations. For the two atoms of monomer 1, that is for $i = 1$ and *a*:

$$\mathbf{a}_i(\theta_1, \theta_2, \phi, R, r_1, r_2) = S^{-1}(\pi/2, \theta_1, \phi/2 - \pi/2) \cdot \mathbf{a}_i^0(r_1) + \frac{R}{2}\mathbf{k}, \quad (2)$$

where $\mathbf{k}$ is the unit vector along the z-axis and $\mathbf{a}_i^0(r)$, with $i = 1$ and *a*, are the position vectors of the hydrogen and iodine atoms of an HI molecule parallel to the z-axis, with an r bond length, such that its center of mass is located at the origin of the molecule-fixed axis system. The $\mathbf{a}_i^0(r)$ position vectors have a nonvanishing z-component equal to $-rm_I/(m_H + m_I)$ and $+rm_H/(m_H + m_I)$ for $i = 1$ and *a*, respectively. The rotation in Eq. (2) can also be written as $C_z(\phi/2)\cdot C_x(\theta_1)$. Similarly for the two atoms of monomer 2, that is for $i = 2$ and *b*:

$$\mathbf{a}_i(\theta_1, \theta_2, \phi, R, r_1, r_2) = S^{-1}(\pi/2, \theta_2, -\phi/2 - \pi/2) \cdot \mathbf{a}_i^0(r_2) - \frac{R}{2}\mathbf{k}, \quad (3)$$

where $\mathbf{a}_i^0(r)$, with $i = 2$ and *b*, is defined as for Eq. (2). The rotation in this equation can also be written as $C_z(-\phi/2)\cdot C_x(\theta_2)$. To avoid redundancies, the two bending angles and the torsional angle appearing in Eqs. (1)–(3) should fulfill the relations:

$$0 \leqslant \theta_1 \leqslant \pi, \quad 0 \leqslant \theta_2 \leqslant \pi, \quad 0 \leqslant \phi \leqslant 2\pi. \quad (4)$$

The choice made in Eqs. (1)–(3) ensures that the molecular center of mass is at the origin of the molecule-fixed *xyz*-axis system. When $\phi = 0$ ($\phi = \pi$) the dimer is planar and both monomers are in the *yz*-plane (*xz*-plane). Fig. 2 illustrates the atom positions for $\theta_1 = 43°$, $\theta_2 = 137°$, and $\phi = 180°$, which are values of the internal angular coordinates corresponding to the C_{2h} geometry minimum of the *ab initio* potential energy surface [38,39]. The choice made in Eqs. (1)–(3) also ensures that the *xyz*-axis system is within a

Table 2
Transformation properties of the coordinates[a] and character table of the permutation-inversion symmetry group of the HI dimer.

	E	$(12)(ab)$	E^*	$(12)(ab)^*$
Internal[b]	θ_1, θ_2	$\pi-\theta_2, \pi-\theta_1$	θ_1, θ_2	$\pi-\theta_2, \pi-\theta_1$
	ϕ	ϕ	$2\pi-\phi$	$2\pi-\phi$
	r_1, r_2	r_2, r_1	r_1, r_2	r_2, r_1
Rotation[c]	χ_d	$\pi-\chi_d$	$\pi-\chi_d$	χ_d
	θ_d	$\pi-\theta_d$	$\pi-\theta_d$	θ_d
	ϕ_d	$\phi_d+\pi$	$\phi_d+\pi$	ϕ_d
A_g	1	1	1	1
A_u	1	1	−1	−1
B_g	1	−1	−1	1
B_u	1	−1	1	−1

[a] The coordinates used for the HI dimer are defined in Eq. (1).
[b] These rows indicate the effects of the symmetry operations on the internal coordinates. The R coordinate does not appear as it is unvariant under all four symmetry operations.
[c] These rows indicate the effects of the symmetry operations on the Eulerian angles χ_d, θ_d, ϕ_d. See text for the equivalent rotations.

few degrees from the principal axis system. More precisely, the x-, y-, and z-axes are almost parallel to the b-, c-, and a-axes, respectively, implying that the I^r representation is used.

The permutation-inversion symmetry group to be used for the HI dimer is isomorphic to the C_{2h} point group and contains four operations: E, $(12)(ab)$, E^*, and $(12)(ab)^*$. The character table of the symmetry group along with the effects of the four operations on the internal coordinates and on the Euler angles are given in Table 2. For the latter, the equivalent rotation [40] to be used for the generating operations $(12)(ab)$ and E^* is $Cy(\pi)$.

4.2. Rotational and hyperfine coupling Hamiltonians

The *ab initio* calculations [38,39] have shown that the potential energy surface displays one minima at $-358.6\ cm^{-1}$ corresponding to a C_{2h} geometry characterized by $\theta_1 = 43°$, $\theta_2 = \pi - \theta_1 = 137°$, $\phi = 180°$, and $R = 4.35$ Å. The two vibrational states involved in the data measured in the present work are the ground vibrational state and the first excited vibrational state of the planar ν_5 geared bending mode. This mode corresponds to the coordinate $\theta_1 + \theta_2 - \pi$ and its first excited vibrational state is the lowest lying vibrational state of the dimer. The ground vibrational state, which will be henceforth denoted $\nu_5 = 0$, and the $\nu_5 = 1$ vibrational state have energies [38,39] of -216.96 and $-199.88\ cm^{-1}$, respectively. It will be assumed that the rotational energy in these two states can be obtained using a usual Watson-type Hamiltonian written, in accordance with Section 4.1, using the I^r representation and the A-reduction:

$$H_{\nu_5} = A^{\nu_5}J_z^2 + B^{\nu_5}J_x^2 + C^{\nu_5}J_y^2 - \Delta_{KK}^{\nu_5}J_z^4 - \Delta_{KJ}^{\nu_5}\mathbf{J}^2J_z^2 - \Delta_{JJ}^{\nu_5}\mathbf{J}^4 - \{\delta_K^{\nu_5}J_z^2 + \delta_J^{\nu_5}\mathbf{J}^2, J_x^2 - J_y^2\}, \quad (5)$$

where $\nu_5 = 0$ and 1; and $\mathbf{J}$, J_x, J_y, and J_z are the total angular momentum and its components in the molecule-fixed axis system.

As stressed in Section 1, the hyperfine electric quadrupole coupling is very strong in the hydrogen iodide molecule. In the HI dimer, quadrupole coupling should therefore be considered and we are led to write a quadrupole coupling hyperfine Hamiltonian [41] which we express with the help of products [42] of irreducible rank 2 tensor operators:

$$H_Q = Q_a^{(2)} \cdot V_a^{(2)} + Q_b^{(2)} \cdot V_b^{(2)}, \quad (6)$$

where $Q_n^{(2)}$, with $n = a$ and b, are the rank 2 tensor operators corresponding to the nuclear quadrupole moment of iodine atoms a and b; and $V_n^{(2)}$, with $n = a$ and b, are the rank 2 tensor operators corresponding to the electric field gradient tensor at iodine atoms a and b. These latter two tensors depend on the six internal coordinates θ_1, θ_2, ϕ, R, r_1, and r_2 defined in Section 4.1. Making use of symmetry adapted operators, the hyperfine coupling Hamiltonian of Eq. (6) can be written in a way more suitable for the evaluation of the hyperfine matrix elements:

$$H_Q = Q_S^{(2)} \cdot V_S^{(2)} + Q_A^{(2)} \cdot V_A^{(2)}, \quad (7)$$

where $Q_S^{(2)}$, $V_S^{(2)}$, $Q_A^{(2)}$, and $V_A^{(2)}$ are four rank 2 tensors operators:

$$\begin{cases} Q_S^{(2)} = Q_a^{(2)} + Q_b^{(2)}, & V_S^{(2)} = (V_a^{(2)} + V_b^{(2)})/2, \\ Q_A^{(2)} = Q_a^{(2)} - Q_b^{(2)}, & V_A^{(2)} = (V_a^{(2)} - V_b^{(2)})/2. \end{cases} \quad (8)$$

Using Table 2, it can be shown easily that laboratory-fixed components of the tensor operators $Q_S^{(2)}$ and $V_S^{(2)}$ ($Q_A^{(2)}$ and $V_A^{(2)}$) belong to the symmetry species A_g (B_u). This leads to several relations involving the Cartesian components of the 3×3 tensors $\mathbf{V}_S$ and $\mathbf{V}_A$ in the molecule-fixed axis system. Four of them are given below as they are needed for the evaluation of the matrix elements of these tensors:

$$V_T(\theta_1, \theta_2, \phi, R, r_1, r_2)_{\alpha\beta} = -V_T(\theta_1, \theta_2, 2\pi - \phi, R, r_1, r_2)_{\alpha\beta}, \quad (9)$$

where $T = S$ and A, and $\alpha\beta = xy$ and yz.

4.3. Symmetry adapted rovibrational–hyperfine wavefunctions

The vibrational wavefunctions arising for the HI dimer depend on the six internal coordinates introduced in Section 4.1. They will be written:

$$\phi_{\nu_5}(\theta_1, \theta_2, \phi, R, r_1, r_2), \quad (10)$$

where $\nu_5 = 0$ and 1. The $\nu_5 = 0$ wavefunction is the ground vibrational state wavefunction and is invariant under any operation of the permutation-inversion symmetry group. The $\nu_5 = 1$ wavefunction has no quantum of energy in the torsional mode. It is not altered by the E^* symmetry operation which changes the sign of the coordinate for the torsional mode: $\phi - \pi$. This wavefunction is changed into its opposite by the $(12)(ab)$ symmetry operation which changes the sign of the coordinate for the geared-type mode: $\theta_1 + \theta_2 - \pi$. These results indicate that the vibrational wavefunctions in Eq. (10) belong to the A_g and B_u symmetry species for $\nu_5 = 0$ and 1, respectively.

The symmetry adapted rotational wavefunctions which will be used for the HI dimer, are the $|JK\gamma\rangle$ defined in Eq. (21) of Ref. [43]. Using Table 2, it can be shown that these wavefunctions belong to the symmetry species A_g (B_g) when $\gamma(-1)^{J+K}$ is +1 (−1).

Symmetry adapted hyperfine wavefunctions are written using the coupled basis set. They are characterized by I the quantum number for the total nuclear spin angular momentum for the two iodine nuclei: $\mathbf{I} = \mathbf{I}_a + \mathbf{I}_b$, by F the quantum number for the total angular momentum: $\mathbf{F} = \mathbf{I} + \mathbf{J}$, and by M_F its projection along the laboratory-fixed Z-axis. These wavefunctions take the following expression:

$$|I_aI_b, I, J, FM_F\rangle, \quad (11)$$

with $0 \leqslant I \leqslant 5$ and $|J - I| \leqslant F \leqslant J + I$. Using Table 2 and taking into account the properties of $3-j$ symbols, it can be shown that the wavefunctions in Eq. (11) belong to the symmetry species A_g for odd I-values and to the symmetry species B_u for even I-values. The total rovibrational–hyperfine symmetry adapted wavefunctions to be used to diagonalize the Hamiltonian matrix will be the product of the three above wavefunctions:

$$\Psi_{I,J,FM_F}^{\nu_5\, r} = \phi_{\nu_5} \times |JK\gamma\rangle \times |I_aI_b, I, J, FM_F\rangle, \quad (12)$$

where r is a shorthand notation for the rotational quantum numbers: J, K, and γ. Table 3 gives the symmetry species of the total

Table 3
Symmetry species[a] of the total wavefunction in Eq. (12).

Γ	v_5	$\gamma(-1)^{J+K}$	I	Γ	v_5	$\gamma(-1)^{J+K}$	I
A_g	0	+1	*Odd*	B_u	1	+1	*Odd*
B_u	0	+1	*Even*	A_g	1	+1	*Even*
B_g	0	−1	*Odd*	A_u	1	−1	*Odd*
A_u	0	−1	*Even*	B_g	1	−1	*Even*

[a] The symmetry species in C_{2h} is given in the column headed Γ as a function of the quantum numbers appearing in the other columns and defined in Section 4.3.

wavefunctions as a function of the quantum numbers appearing in this equation.

4.4. Hamiltonian matrix elements

Matrix elements of the rovibrational and hyperfine coupling Hamiltonians between two total wavefunctions of Eq. (12) characterized by the same value of F and M_F:

$$\left\langle \Psi^{v'5\,r'}_{I'J',FM_F} | H_{VR} + H_Q | \Psi^{v_5\,r}_{IJ,FM_F} \right\rangle, \tag{13}$$

are calculated in this section. It is convenient to distinguish between matrix elements with $\Delta v_5 = 0$ from those with $\Delta v_5 = 1$.

4.4.1. $\Delta v_5 = 0$ matrix elements

This first type of matrix elements contains rovibrational and hyperfine coupling contributions. This latter contribution should be evaluated using Eq. (7.1.6) of Ref. [42] and Eq. (7) of the present paper. For symmetry reasons, only the first term in the latter equation has nonvanishing matrix elements:

$$\begin{aligned}\langle \Psi^{v_5\,r'}_{I'J',FM_F} | H_{VR} + H_Q | \Psi^{v_5\,r}_{IJ,FM_F} \rangle &= E_{v_5}\delta_{I',I}\delta_{J',J}\delta_{K',K}\delta_{\gamma',\gamma} \\ &+ \langle J'K'\gamma' | H_{v_5} | JK\gamma\rangle \delta_{I',I}\delta_{J'J} + (-1)^{I+J'+F}\begin{Bmatrix} F & J' & I' \\ 2 & I & J \end{Bmatrix} \\ &\times \langle I_a I_b, I' \| Q_S^{(2)} \| I_a I_b, I\rangle \langle v_5, J'K'\gamma' \| v_S^{(2)} \| v_5, JK\gamma\rangle \end{aligned} \tag{14}$$

where E_{v_5} is the vibrational energy; H_{v_5} is the Watson-type Hamiltonian defined in Eq. (5); and $Q_S^{(2)}$ and $V_S^{(2)}$ are the tensor operators defined in Eq. (8). Evaluation of the reduced matrix element of the hyperfine $Q_S^{(2)}$ operator can be performed using Eqs. (7.1.7) and (7.1.8) of Ref. [42]:

$$\begin{aligned}\langle I_a I_b, I' \| Q_S^{(2)} \| I_a I_b, I\rangle &= (-1)^{I_a+I_b+I}\sqrt{(2I+1)(2I'+1)} \\ &\times \left[\begin{Bmatrix} I_a & I' & I_b \\ I & I_a & 2 \end{Bmatrix} \langle I_a \| Q_a^{(2)} \| I_a\rangle \begin{Bmatrix} I_b & I' & I_a \\ I & I_b & 2 \end{Bmatrix} \langle I_b \| Q_b^{(2)} \| I_b\rangle \right], \end{aligned} \tag{15}$$

where $I_a = I_b = \frac{5}{2}$ and $\langle I_a \| Q_a^{(2)} \| I_a\rangle = \langle I_b \| Q_b^{(2)} \| I_b\rangle$ is given in Eqs. (16) and (17) of Ref. [41] and involves the electric quadrupole moment of the iodine atom eQ. Evaluation of the reduced matrix element of the rovibrational $V_S^{(2)}$ operator involves replacing the symmetry adapted rotational wavefunctions by symmetric top rotational wavefunctions. Using the expression of the symmetry adapted rotational wavefunctions given in Eq. (21) of Ref. [43], we obtain:

$$\begin{aligned}\langle v'_5, J'K'\gamma' \| V_A^{(2)} \| v_5, JK\gamma\rangle &= \frac{1}{2}\Big[\langle v'_5, J', K' \| V_A^{(2)} \| v_5, J, K\rangle + \gamma \langle v'_5, J', \\ &K' \| V_A^{(2)} \| v_5, J, -K\rangle + \gamma' \langle v'_5, J', -K' \| V_A^{(2)} \| v_5, J, K\rangle \\ &+ \gamma\gamma' \langle v'_5, J', -K' \| V_A^{(2)} \| v_5, J, -K\rangle \Big], \end{aligned} \tag{16}$$

where the term on the right-hand side must be divided by $\sqrt{2}$ if either K' or K is equal to zero, but not both; if both K' and K are equal to zero, a division by 2 must be performed. Any of the above reduced matrix elements can be calculated using Eq. (3.24) of Ref. [44]:

$$\begin{aligned}\langle v'_5, J'K' \| V_A^{(2)} \| v_5, J, K\rangle &= [(2J+1)(2J'+1)]^{1/2} \times (-1)^{J'-K'} \\ &\times \sum_{q=-2}^{2} \begin{pmatrix} J & J' & 2 \\ K & -K' & q \end{pmatrix} \langle \phi_{v'_5} | V_{Aq}^{(2)} | \phi_{v_5}\rangle, \end{aligned} \tag{17}$$

where $V_{Sq}^{(2)}$, with $-2 \leqslant q \leqslant +2$, are the components of the rank 2 tensor $V_S^{(2)}$. These components can be expressed in terms of the Cartesian coordinates of this tensor with the help of Eq. (28) of Ref. [41]:

$$\begin{aligned}\langle \phi_{v_5} | V_{S0}^{(2)} | \phi_{v_5}\rangle &= \langle \phi_{v_5} | V_{Szz} | \phi_{v_5}\rangle / 2 \\ \langle \phi_{v_5} | V_{S\pm2}^{(2)} | \phi_{v_5}\rangle &= \pm \langle \phi_{v_5} | V_{Sxz} | \phi_{v_5}\rangle / \sqrt{6} \\ \langle \phi_{v_5} | V_{S\pm2}^{(2)} | \phi_{v_5}\rangle &= \pm \langle \phi_{v_5} | V_{Sxx} - V_{Syy} | \phi_{v_5}\rangle / \sqrt{24} \end{aligned} \tag{18}$$

In these equations the components V_{Sxy} and V_{Syz} do not appear as, in agreement with Eq. (9), they have vanishing matrix elements.

4.4.2. $\Delta v_5 = 1$ matrix elements

This second type of matrix elements contains a contribution from the hyperfine coupling Hamiltonian only. This contribution is also evaluated using Eq. (7.1.6) of Ref. [43] and Eq. (7) of the present Letter. For symmetry reason, only the second term in the latter equation has nonvanishing matrix elements:

$$\begin{aligned}\langle \Psi^{v'_5\,r'}_{I'J',FM_F} | H_{VR} + H_Q | \Psi^{v_5\,r}_{IJ,FM_F} \rangle &= (-1)^{I+J'+F}\begin{Bmatrix} F & J' & I' \\ 2 & I & J \end{Bmatrix} \\ &\times \langle I_a I_b, I \Big\| Q_A^{(2)} \Big\| I_a I_b, I\rangle \langle v'_5, J'K'\gamma' \Big\| V_A^{(2)} \Big\| v_5, JK\gamma\rangle, \end{aligned} \tag{19}$$

where and $Q_A^{(2)}$ and $V_A^{(2)}$ are the tensor operators defined in Eqs. (8). Evaluation of the reduced matrix element of the hyperfine former operator can be performed as for Eq. (15) and changing the sign for the contribution from the b iodine atom. As in the previous section, evaluation of the reduced matrix element of the rovibrational $V_A^{(2)}$ operator involves replacing the symmetry adapted rotational wavefunctions by symmetric top rotational wavefunctions. Using the expression of the symmetry adapted rotational wavefunctions given in Eq. (21) of Ref. [43], we obtain:

$$\begin{aligned}\langle v'_5 J'K'\gamma' \| V_S^{(2)} \| v'_5 J\ K\ \gamma\rangle &= \frac{1}{2}[\langle v'_5 J', K' \| V_S^{(2)} \| v_5, J, K\rangle \\ &+ \gamma \langle v'_5 J', K' \| V_S^{(2)} \| v_5, J, -K\rangle + \gamma' \langle v'_5 J', -K' \| V_S^{(2)} \| v_5, J, K\rangle \\ &+ \gamma\gamma' \langle v'_5 J', -K' \| V_S^{(2)} \| v_5, J, -K\rangle], \end{aligned} \tag{20}$$

where the term on the right-hand side must be divided by $\sqrt{2}$ if either K' or K is equal to zero, but not both; if both K' and K are equal to zero, a division by 2 must be performed. Any of the above reduced matrix elements can be calculated using Eq. (3.24) of Ref. [44]:

$$\begin{aligned}\langle v'_5, J'K' \| V_A^{(2)} \| v_5, JK\rangle &= [(2J+1)(2J'+1)]^{1/2} \times (-1)^{J'-K'} \\ &\times \sum_{q=-2}^{2} \begin{pmatrix} J & J' & 2 \\ K & -K' & q \end{pmatrix} \langle \phi_{v'_5} | V_{Aq}^{(2)} | \phi_{v_5}\rangle, \end{aligned} \tag{21}$$

where $V_{Aq}^{(2)}$, with $-2 \leqslant q \leqslant +2$, are the components of the rank 2 tensor $V_A^{(2)}$. These components can be expressed in terms of the Cartesian coordinates of the $\mathbf{V}_A$ tensor with the help of Eq. (28) of Ref. [41]. We obtain:

$$\begin{aligned}\langle \phi_{v'_5} | V_{A0}^{(2)} | \phi_{v_5}\rangle &= \langle \phi_{v_5} | V_{Azz} | \phi_{v_5}\rangle / 2 \\ \langle \phi_{v'_5} | V_{A\pm1}^{(2)} | \phi_{v_5}\rangle &= \mp \langle \phi_{v'_5} | V_{Axz} | \phi_{v_5}\rangle / \sqrt{6} \\ \langle \phi_{v'_5} | V_{A\pm2}^{(2)} | \phi_{v_5}\rangle &= \mp \langle \phi_{v'_5} | V_{Axx} - V_{Ayy} | \phi_{v_5}\rangle / \sqrt{24}. \end{aligned} \tag{22}$$

In these equations the components V_{Axy} and V_{Ayz} do not appear as, in agreement with Eq. (9), they have vanishing matrix elements.

4.5. Rovibrational–hyperfine energy level calculation

The Hamiltonian matrix is setup and diagonalized using as basis set functions the symmetry adapted wavefunctions of Eq. (12) for a given symmetry species and a given F value. Table 3 should be used to obtain allowed values for v_5, γ, and I. In addition to that, the values of J and I should satisfy the triangle relation for angular momenta addition. The number of basis-set wavefunctions increases quite rapidly with F. When $F = 5$, it is equal to 198 for all symmetry species. In order to reduce the size of the Hamiltonian matrix for large F-values, only basis-set wavefunctions with $K \leqslant 2$ were selected. This leads to a Hamiltonian matrix that cannot be bigger than a 90×90 matrix.

Hamiltonian hyperfine matrix elements should be obtained using Eqs. (14)–(22). They depend on the quadrupole moment eQ arising from the reduced matrix elements of $Q_S^{(2)}$ and $Q_A^{(2)}$ and on the six tensor components defined in Eqs. (18) and (22). These matrix elements can be conveniently expressed with the help of two effective quadrupole coupling tensors:

$$\chi(S)_{\alpha\beta}^{v_5} = eQ\langle\phi_{v_5}|V_{S\alpha\beta}|\phi_{v_5}\rangle, \tag{23}$$

where $v_5 = 0$ and 1, and:

$$\chi(A)_{\alpha\beta} = eQ\langle\phi_{v_5=0}|V_{A\alpha\beta}|\phi_{v_5=1}\rangle, \tag{24}$$

For these two equations, $\alpha\beta = xx$, yy, and xz. Table 4 gives calculated values for various components of the effective quadrupole coupling tensors in Eqs. (23) and (24). The vibrational matrix elements in these equations were computed using the vibrational wavefunctions retrieved from the dimer *ab initio* potential energy surface [38,39]. It was assumed that the value of the effective quadrupole coupling constant eQq for each subunit is the same as that of an isolated hydrogen iodide molecule: −1828.059 MHz, as obtained by Terahertz spectroscopy by Chance et al. [28].

Rovibrational–hyperfine levels were assigned with the good quantum number F and with the four approximate quantum numbers I, J, K_a and K_c. Values for these quantum numbers were obtained assuming that the ordering of the energy levels is not altered by the nondiagonal matrix elements of the Hamiltonian matrix.

5. Analysis

The frequencies measured in the present work were introduced in a least squares fitting program in which the energy level calculation was performed using the theoretical approach described in the previous section. As the observed data only involve a-type rovibrational transitions with $K_a = 0$, it was not possible to obtain values for all the zeroth-order rotational constants in Eq. (5). For both vibrational states, only $(B^{v5} + C^{v5})/2$ and could be determined. The rotational constant A^{v5} was constrained to the value calculated with the *ab initio* surface [38,39]. For the same reason, the quadrupole coupling constants $\chi(S)_{xx}^{v_5} - \chi(S)_{yy}^{v_5}$, with $v_5 = 0$ and 1, and $\chi(A)_{xx} - \chi(A)_{yy}$ were ill-defined and were constrained to the values given in Table 4. Table 1 lists assignments, frequencies, and observed minus calculated residuals for the 345 transitions recorded in this work. As indicated by this table, two transitions were excluded from the analysis as they displayed residuals much larger than the experimental uncertainty on the line frequency. The root mean square deviation of the observed minus calculated difference is 18 kHz. Table 5 gives the values obtained for the spectroscopic parameters. Parameters that do not appear in this table were set to zero.

The agreement between the values given in Table 5 and those given in Table 4 is quite satisfactory for the constants $\chi(S)_{xx}^{v_5} + \chi(S)_{yy}^{v_5}$, with $v_5 = 0$ and 1, which have an uncertainty much smaller than 1 MHz. The discrepancy is 1.2 MHz for $v_5 = 0$ and 2.2 MHz for $v_5 = 1$. For the similar constant $\chi(A)_{xx} + \chi(A)_{yy}$, the agreement is much less satisfactory and this is expected as this constant is involved in nondiagonal matrix elements only and has a much larger uncertainty than the two previous ones. For the constants $\chi(S)_{xz}^{v_5}$, with $v_5 = 0$ and 1, and $\chi(A)_{xz}$, the agreement is not satisfactory either. In this case this stems from the fact that the present data set only involves transitions with $K_a = 0$.

Table 4
Calculated[a] values for the effective quadrupole coupling tensors[b] components.

Component	$v_5 = 0$	$v_5 = 1$
$\chi(S)_{xx}^{v_5}$	−238.0	96.5
$\chi(S)_{yy}^{v_5}$	626.6	274.8
$\chi(S)_{xz}^{v_5}$	−875.2	−379.6
$\chi(S)_{xx}^{v_5} + \chi(S)_{yy}^{v_5}$	388.6	371.3
$\chi(S)_{xx}^{v_5} - \chi(S)_{yy}^{v_5}$	−864.6	−178.3
$\chi(A)_{xx}$	448.8	
$\chi(A)_{yy}$	237.0	
$\chi(A)_{xz}$	−128.6	
$\chi(A)_{xx} + \chi(A)_{yy}$	685.9	
$\chi(A)_{xx} - \chi(A)_{yy}$	211.8	

[a] Calculated values are in MHz.
[b] The effective quadrupole coupling tensors are defined in Eqs. (23) and (24).

Table 5
Spectroscopic parameters[a] obtained for the HI dimer.

Parameter	$v_5 = 0$	$v_5 = 1$
E^{v5}	0.0[b]	511 931.090(14)
A^{v5}	232 000.0[b]	232 000.0[b]
$(B^{v5} + C^{v5})/2$	378.299 90(42)	370.810 99(29)
$B^{v5} - C^{v5}$	2.411(1700)	10.647(7900)
$\Delta_{IJ}^{v_5} \times 10^3$	0.364 01(810)	0.292 39(2300)
$\chi(S)_{xx}^{v_5} + \chi(S)_{yy}^{v_5}$	389.861 03(900)	377.464 85(990)
$\chi(S)_{xx}^{v_5} - \chi(S)_{yy}^{v_5}$	−864.6[b]	−178.3[b]
$\chi(S)_{xz}^{v_5}$	−778.80(610)	−175.4(380)
$\chi(A)_{xx} + \chi(A)_{yy}$	559.09(910)	
$\chi(A)_{xx} - \chi(A)_{yy}$	211.8[b]	
$\chi(A)_{xz}$	−146.7(490)	

[a] Parameters are in MHz. For the fitted parameters, numbers in parentheses are one standard deviation in the same units as the last digit.
[b] Constrained value.

6. Conclusion

The submillimeter spectrum of the geared bending vibration in HI dimer has been recorded in a supersonic jet expansion at an effective temperature of 1.2 K. The resolution, on the order of 50 kHz, achieved by the experimental setup allowed us to fully resolve the iodine-iodine quadrupole structure for low-J transitions. A theoretical approach has been developed to account for the coupling between the large amplitude geared bending vibration and the large hyperfine quadrupole coupling. The theoretical approach involves building an effective rovibrational–hyperfine Hamiltonian using symmetry considerations. Hyperfine matrix elements of this Hamiltonian with $\Delta J \leqslant 2$ are evaluated between as well as within the ground and the first excited vibrational state of the geared bending vibration ($v_5 = 1$). This enabled the fit of the experimental data with a standard deviation of 18 kHz. Although this value still is significantly larger than the accuracy of the individually measured transitions, estimated to be 2 kHz, the results of the analysis are consistent with those obtained using an *ab initio* potential energy surface [38,39]. This is emphasized by Tables 4 and 5 which show that there is a fairly good agreement between experimental

and calculated values for most spectroscopic constants. When quadrupole coupling matrix elements between the ground and the $v_5 = 1$ states are ignored, setting all components of the $\chi(A)$ tensor in Table 5, the standard deviation of the observed minus calculated difference rises to 36 kHz and this further confirms that the upper vibrational state of the observed band indeed has the symmetry species expected for the $v_5 = 1$ excited vibrational state. This also confirms that the HI dimer is among the few molecular systems [36] for which hyperfine effects across different vibrational states could be evidenced. The energy level calculation for this unusual situation cannot be carried out using Pickett's SPFIT program [35]. Using some of the well defined spectroscopic constants in Table 5 for the ground vibrational state yields the following averaged geometry parameters: $R_{cm} = 4.56372(1)$ Å and $\theta = 46.405(1)^\circ$ which can be compared with corresponding values of 3.7849(1) Å and 48.050° for $(HCl)_2$, and 4.1077(1) Å and 47.280° for $(HBr)_2$.

The issue of whether the potential of HI dimer is similar to other members of the homologous series or not is unresolved. The comparison between observed and calculated quadrupole coupling constants is still not completely satisfactory partially because of the current lack of $K_a > 0$ data. The question of a barrier to tunneling interconversion and an L-shaped global minimum structure or whether the barrier is below the ground state or even non-existent and thus being consistent in the latter case with a single global minimum and a symmetric dimer structure must await further investigation.

Acknowledgement

We are grateful to the National Science Foundation and the Laboratory Submm/THz.Sc&Tech Texas A&M University for financial support for this research. J.W. Bevan expresses gratitude to the Robert A. Welch Foundation (Grant A-747) for financial support for fellowships for B.A. McElmurry and F.F. Willaert.

References

[1] J. Castillo-Chara, A.L. McIntosh, Z. Wang, R.R. Lucchese, J.W. Bevan, J. Chem. Phys. 120 (2004) 10426.
[2] M.J. Elrod, R.J. Saykally, J. Chem. Phys. 103 (1995) 921.
[3] M.J. Elrod, R.J. Saykally, J. Chem. Phys. 103 (1995) 933.
[4] X.T. Wu, E.F. Hayes, A.B. McCoy, J. Chem. Phys. 110 (1999) 2365.
[5] X.T. Wu, A.B. McCoy, E.F. Hayes, J. Chem. Phys. 110 (1999) 2354.
[6] T.R. Dyke, B.J. Howard, W. Klemperer, J. Chem. Phys. 56 (1972) 2442.
[7] H.C. Chang, W. Klemperer, J. Chem. Phys. 98 (1993) 9266.
[8] W. Klopper, H.P. Luthi, Mol. Phys. 96 (1999) 559.
[9] W. Klopper, M. Quack, M.A. Suhm, J. Chem. Phys. 108 (1998) 10096.
[10] M.D. Schuder, C.M. Lovejoy, R. Lascola, D.J. Nesbitt, J. Chem. Phys. 99 (1993) 4346.
[11] Y.H. Qiu, Z. Bacic, J. Chem. Phys. 106 (1997) 2158.
[12] Y.H. Qiu, J.Z.H. Zhang, Z. Bacic, J. Chem. Phys. 108 (1998) 4804.
[13] W. Chen, A.R.H. Walker, S.E. Novick, F.M. Tao, J. Chem. Phys. 106 (1997) 6240.
[14] B.A. McElmurry, R.R. Lucchese, J.W. Bevan, S.P. Belov, I.I. Leonov, Chem. Phys. Lett. 407 (2005) 40.
[15] J. Zhang, M. Dulligan, J. Segall, Y. Wen, C. Wittig, J. Phys. Chem. 99 (1995) 13680.
[16] M.A. Young, J. Chem. Phys. 102 (1995) 7925.
[17] K.L. Randall, D.J. Donaldson, J. Phys. Chem. 99 (1995) 6763.
[18] Y. Hannachi, B. Silvi, THEOCHEM – J. Mol. Struct. 59 (1989) 483.
[19] Z. Latajka, S. Scheiner, Chem. Phys. 216 (1997) 37.
[20] M.T. Bowers, W.H. Flygare, J. Chem. Phys. 44 (1966) 1389.
[21] A.J. Barnes, J.B. Davies, H.E. Hallam, G.f. Scrimsha, G.C. Hayward, R.C. Milward, J. Chem. Soc. D – Chem. Commun. (1969) 1089.
[22] D. Maillard, A. Schriver, J.P. Perchard, C. Girardet, J. Chem. Phys. 71 (1979) 505.
[23] A. Engdahl, B. Nelander, J. Phys. Chem. 90 (1986) 6118.
[24] A.L. McIntosh, Z. Wang, R.R. Lucchese, J.W. Bevan, Chem. Phys. Lett. 328 (2000) 153.
[25] A.L. McIntosh, Z. Wang, R.R. Lucchese, J.W. Bevan, Infrared Phys. Technol. 45 (2004) 301.
[26] B.A. McElmurry, R.R. Lucchese, J.W. Bevan, S.P. Belov, PCCP 6 (2004) 5318.
[27] J.B. Simpson, J.G. Smith, D.H. Whiffen, J. Mol. Spectrosc. 44 (1972) 558.
[28] K.V. Chance, T.D. Varberg, K. Park, L.R. Zink, J. Mol. Spectrosc. 162 (1993) 120.
[29] G.R. Hanes, J. Lapierre, P.R. Bunker, K.C. Shotton, J. Mol. Spectrosc. 39 (1971) 506.
[30] C.H. Townes, A.L. Schawlow, Microwave Spectroscopy, McGraw-Hill Book Company, New York, 1955.
[31] H.S. Gutowsky, C. Chuang, J.D. Keen, T.D. Klots, T. Emilsson, J. Chem. Phys. 83 (1985) 2070.
[32] J.A. Coxon, P.G. Hajigeorgiou, J. Mol. Spectrosc. 142 (1990) 254.
[33] P.R. Bunker, V.C. Epa, P. Jensen, A. Karpfen, J. Mol. Spectrosc. 146 (1991) 200.
[34] B.A. McElmurry, R.R. Lucchese, J.W. Bevan, I.I. Leonov, S.P. Belov, A.C. Legon, J. Chem. Phys. 119 (2003) 10687.
[35] H.M. Pickett, J. Mol. Spectrosc. 148 (1991) 371.
[36] I. Merke, L.H. Coudert, J. Mol. Spectrosc. 237 (2006) 174.
[37] E.B. Wilson, J.C. Decius, P.C. Cross, McGraw-Hill Book Company Inc., New York, Toronto, London, 1955.
[38] F.F. Willaert, B.A. McElmurry, R.R. Lucchese, J.W. Bevan, Chem. Phys. Lett. 460 (2008) 525.
[39] F.F. Willaert, B.A. McElmurry, R.R. Lucchese, J.W. Bevan, J. Chem. Phys. (in press).
[40] P.R. Bunker, Molecular Symmetry and Spectroscopy, Academic Press, New York, 1979.
[41] R.L. Cook, F.C. De Lucia, Am. J. Phys. 39 (1971) 1433.
[42] A.R. Edmonds, Angular Momentum in Quantum Mechanics, Princeton University Press, Princeton, NJ, 1960.
[43] L.H. Coudert, J. Mol. Spectrosc. 154 (1992) 427.
[44] K.K. Svidzinskii, in: D.V. Skobel'tsyn (Ed.), Soviet Maser Research, 1964.